Full Paper

Wiley Online Library

ELECTROANALYSIS

DOI: 10.1002/elan.201900615

Molecular Recognition of Phenylalanine Enantiomers onto a Solid Surface Modified with Electropolymerized Pyrrole-β-Cyclodextrin Conjugate

Tatiana V. Shishkanova,*[a] Nina Habanová,[a] Michal Řezanka,[b] Gabriela Broncová,[a] Přemysl Fitl,[c] Martin Vrňata,[c] and Pavel Matějka[d]

Abstract: We report the electrochemical deposition of a β-cyclodextrin pyrrole conjugate (Py-β-CD) on an electrode surface including i) characterization based on surface-enhanced Raman scattering and field-emission scanning electron microscopy; ii) studies of the molecular recognition of enantiomers of phenylalanine methyl ester hydrochlorides (Phe) based on linear sweep voltammetry and a quartz crystal microbalance. The PPy-β-CD polymeric layer on a metallic substrate is distinguished by its inhomogeneity, in which both highly ordered β-CD units and highly disordered polymer chains are observed. The voltammetric recognition results showed that PPy-β-CD exhibited a higher sensitivity for D-Phe $(138\pm15)\times10^3$ than for L-Phe $(6\pm1)\times10^3$ within the concentration range 0.1–0.75 mM (n = 3) despite the differences in the polymer arrangement on the surface. A possible mechanism of molecular recognition of phenylalanine enantiomers is discussed.

Keywords: β-cyclodextrin pyrrole conjugate · electrochemical polymerization · enantiomer recognition · voltammetry · quartz crystal microbalance

1 Introduction

Cyclodextrins (CDs) are able to form inclusion complexes with a number of organic or inorganic analytes, whose stability depends on non-covalent interactions [1] as well as the steric properties of the CD cavity [2]. The complexing properties of CDs are interesting with respect to the development of sensors [3–4]. In order to transfer the recognizing process onto the sensor surface, various approaches for anchoring CD molecules have been proposed and used. β-CDs can be deposited on an electrode surface by polycondensation with dialdehyde [5–7], covalent linking to hyperbranched poly(acrylic acid) films capped with a chemically grafted, ultrathin polyamine layer [8] or nucleophilic attack of the highly oxidized conducting poly(*N*-acetylaniline) polymer by the hydroxyl group of β-CD [9]. Electrochemical polymerization is another surface modification option. Zhang et al. [10] modified a carbon paste electrode with β-CD mixed with L-Arg using electrochemical polymerization. A number of authors described the attachment of β-CD onto the electrode surface during the electrochemical polymerization of pyrrole or aniline by doping them with substituted CDs as counter-anions (sulfonated CD) [11–13]. There were attempts to prepare the composite films based on functionalized poly(pyrrole/β-cyclodextrin) using electropolymerization of a 20:1 mixture of β-CD and the pyrrole monomer [14]. An alternative way to attach β-CD onto the electrode surface can be based on the electrochemical polymerization of β-CD derivatives bearing polymerizable units. The polymerizable unit could be a suitable pyrrole which can guarantee the stability of the polymer in both air and water [15]. In this case, it is interesting to look into the contribution of nonspecific and specific interactions during the process of molecular recognition occurring at the solid-liquid interface.

Here we examine the electrochemical deposition, characterization and recognition properties of a solid surface modified with a poly(pyrrole-β-cyclodextrin conjugate) (PPy-β-CD) towards phenylalanine methyl ester hydrochlorides (Phe).

[a] T. V. Shishkanova, N. Habanová, G. Broncová
Department of Analytical Chemistry, University of Chemistry and Technology Prague, Technická 5, 166 28 Prague 6, Czech Republic
E-mail: tatiana.shishkanova@vscht.cz
shishkat@yahoo.com
[b] M. Řezanka
Department of Nanomaterials in Natural Science, Institute for Nanomaterials, Advanced Technologies and Innovation, Technical University of Liberec, Studentská 1402/2, 461 17 Liberec, Czech Republic
[c] P. Fitl, M. Vrňata
Department of Physics and Measurements, University of Chemical Technology Prague, Technická 5, 166 28 Prague 6, Czech Republic
[d] P. Matějka
Department of Physical Chemistry, University of Chemistry and Technology in Prague, Technická 5, 16628 Prague 6, Czech Republic

Supporting information for this article is available on the WWW under https://doi.org/10.1002/elan.201900615

2 Materials and Methods

2.1 Materials

The following chemicals were used for the experiments: a pyrrole-β-cyclodextrin conjugate (Py-β-CD, Figure 1) was synthesized as described previously in [16], pyrrole (Py, Aldrich, USA), lithium perchlorate (Aldrich, USA), potassium hexacyanoferrate(II) and hexacyanoferrate (III) (Lachema, Czech Republic), potassium chloride (Eutech, Netherlands), L-phenylalanine methyl ester hydrochloride (L-Phe, Fluka, Switzerland) and D-phenylalanine methyl ester hydrochloride (D-Phe, Fluka, Switzerland). Prior to use, pyrrole was distilled repeatedly under vacuum until a colourless liquid was obtained. The distilled monomer was stored in the absence of light. The aqueous solutions were prepared with doubly distilled and demineralised water for electrochemical and spectroscopic measurements, respectively.

2.2 Electrochemical Modification of Electrode Surface

Electrochemical modifications of electrode surfaces were performed using cyclic voltammetry (CV) with a Palmsens 3 (PalmSens BV, Netherlands) in a three-electrode system. The working electrodes used were a glassy carbon electrode (GCE) (Electrochemical detectors, Czech Republic), gilded platinum plate (Pt/Au) and chrome/gold (Cr/Au) coated quartz crystals (Stanford Research Systems) for voltammetric, spectroscopic and quartz crystal microbalance (QCM) measurements, respectively. Ag/AgCl (3 M KCl) and a Pt foil were served as the reference and the counter electrodes, respectively.

Electrochemical deposition of Py-β-CD was carried out onto the surfaces of each working electrode from the supporting electrolyte with 1.85 mM Py-β-CD and 0.1 M $LiClO_4$: the potential window was from 0.0 V up to 1.8 V, with a scan rate of 25 mV/s, 14 cycles. For comparison purposes, we conducted the electrochemical deposition of a native pyrrole on the surfaces of GCE from the supporting electrolyte with 0.14 mM Py and 0.1 M $LiClO_4$. Before each modification, the surface of GCE was primarily cleaned mechanically using filter paper and then treated electrochemically by cycling the potential from

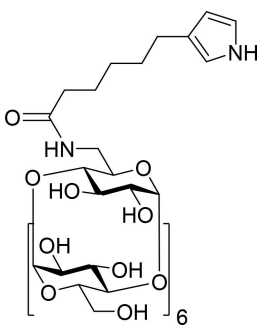

Fig. 1. Structure of a pyrrole-β-cyclodextrin conjugate used in this study.

−0.3 to 1.8 V in 0.5 M H_2SO_4 and rinsed with doubly distilled water.

2.3 Characterization of the Electrochemically Modified Electrode Surface

Surface-enhanced Raman scattering (SERS) measurements were carried out on a gilded platinum (Pt/Au) plate prepared according to [17]. Surface-enhanced Raman spectra were collected in an FT-Raman spectrometer (FT-NIR spectrometer EQUINOX 55, Raman module FRA 106/S, Nd:YAG laser (excitation line 1064 nm, laser power ca. 300 mW) with a Ge diode detector cooled with liquid nitrogen (Bruker Optics)). A standard 4 cm^{-1} spectral resolution was used for all data accumulation. 2048 scans were co-added to obtain spectra of a reasonable S/N ratio. The FT-Raman spectrometer was equipped with a thin-layer chromatography (TLC) mapping stage (Bruker Optics), 8 points were selected to perform a simple spectral mapping. The distance between points was set to 500 µm, because the diameter of the laser beam was ca. 300 µm. Collected spectra of modified Pt/Au-plate were processed in the software package OMNIC 9 (Thermo Scientific, USA).

The morphology studies were carried out by field-emission scanning electron microscopy (FE-SEM Mira, Tescan Orsay Holding, a.s.) using an in-beam secondary electron detector and an accelerating voltage of 10 kV on the Cr/Au surface. Before each measurement, the tested Au surfaces were rinsed in demineralized water and dried at room temperature. Imaging of the bare and PPy-β-CD-modified electrode (Cr/Au) surface was additionally performed by means of AFM and C-AFM Bruker Dimension Icon microscope. The AFM scanning was done using two types of tips namely, Bruker scan asyst air (tip diameter 2 nm, spring constant 0.4 N/m) and Bruker scm-tip conductive tips covered by platinum/iridium (diameter 20 nm, spring constant 2.8 N/m).

2.4 Phenylalanine Methyl Ester Enantiomers Binding Studies

The linear sweep voltammetric (LSV) measurements were performed at bare, PPy- and PPy-β-CD-modified GCE (0.28 cm^2) with the supporting electrolyte (5.0 mM $K_3[Fe(CN)_6]/K_4[Fe(CN)_6]$ (1:1) in 0.1 M $LiClO_4$) in the absence and presence of the amino acid methyl ester hydrochloride in question using a Palmsens 3 device over the potential range of −0.5 to +1.4 V at a scan rate of 100 mV/s. Before each LSV measurement, the supporting electrolyte was purged with N_2. To estimate the sensitivity of the experimental electrodes and at the same time eliminate electrode-to-electrode variation in the background signal, we used the following equation:

$$Response = [(I - I_0)/(I_0)] \times 100\%,$$

where I_0 and I were the current response of the tested GCEs recorded in the supporting electrolyte before and after adding the different concentrations of amino acid methyl ester hydrochlorides.

The QCM experiments were carried out at bare and PPy-β-CD-modified quartz crystals (AT-cut, 1-inch diameter, base frequency 5 MHz, Cr/Au electrodes, polished surface) using a QCM200 equipped with a Kylar QCM head (SRS Stanford Research Systems, USA). Before application, the quartz crystals were purified with piranha solution and rinsed with demineralised water. Before starting the QCM measurements, the solutions were degassed and stabilised to the temperature of the QCM200 probe head. The frequency was recorded with a resolution of 0.1 Hz. Mass changes were computed using the Sauerbrey equation.

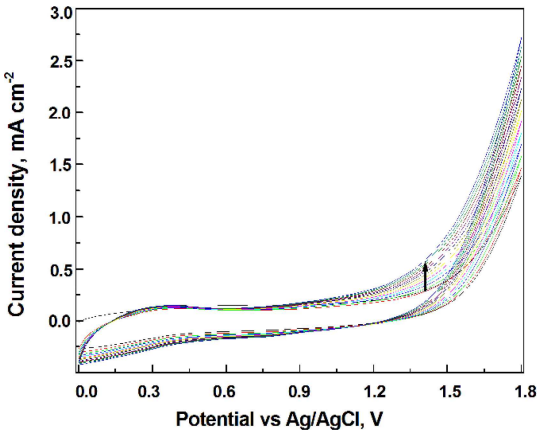

Fig. 2. Cyclic voltammograms of electrochemical polymerization of pyrrole-β-cyclodextrin conjugate in 0.1 M $LiClO_4$ aqueous supporting electrolyte onto the surface of glassy carbon electrode.

3 Results and Discussion

3.1 Electrochemical Modification of Electrode Surface

Electrochemical polymerizations of Py-β-CD were performed onto the surface of the GCE using cyclic voltammetry (Figure 2). The polymerization process of Py-β-CD proceeded with difficulty. Recently, the steric and electronic influence of various substituents on the electropolymerization of five-membered heterocycles were extensively discussed by Lemaire et al. [18] and Waltman [19]. The oxidation process of Py-β-CD was probably significantly affected by the steric hindrance of the bulky β-CD cavity. The bulky substituents attached onto polymerizable units (β-cyclodextrin pyrrole conjugate) or present in the polymerization system are able to reduce the rate of polymer formation. Taking into account this fact, the potential was swept between 0.0 V up to 1.8 V at a scan rate of 25 mV/s [20–21]. The increase in the currents occurring at 1.5 V after 7 cycles during the electrochemical oxidation of PPy-β-CD implies that the polymer was deposited onto the GCE surface. The electrosynthesis was stopped after 14 cycles when the current changes were not observed. An increasing current at 1.5 V was recently observed by Arjomandi et al. during the electrochemical oxidation of pyrrole and 2,6-dimethyl-β-cyclodextrin complex and was taken as confirmation of the formation of the polymeric layer onto the GCE surface [22].

3.2 Characterization of the Electrochemically Modified Electrode Surface

Surface-enhanced Raman scattering (SERS) allows the observation of structural details of films with very small thicknesses deposited on the enhancing substrates. To confirm the formation of the polymer derived from Py-β-CD, the SERS spectra of the monomer (Figure 3A) and

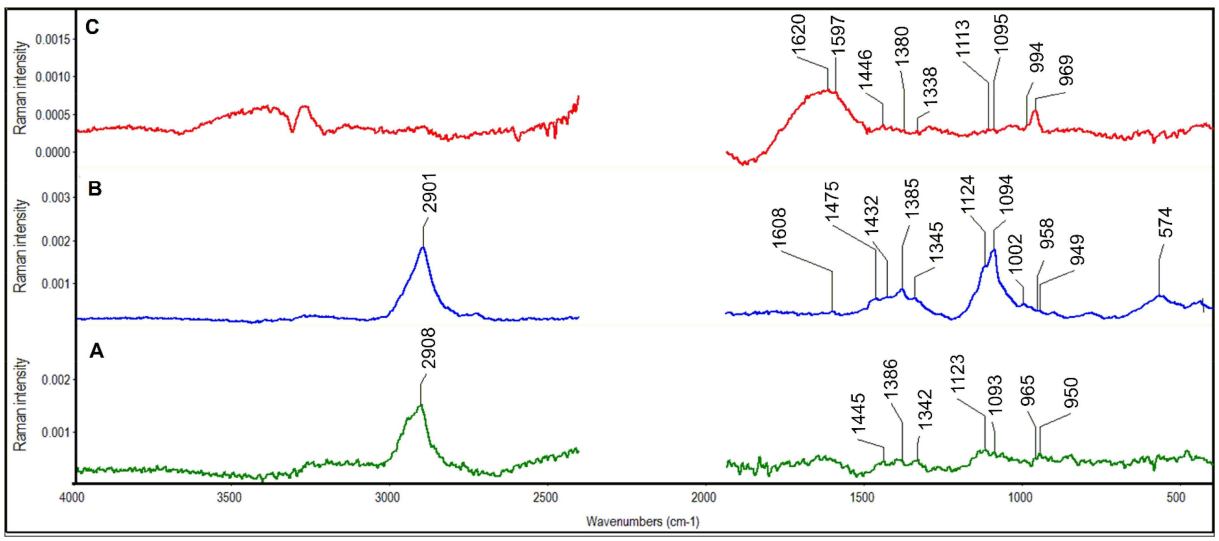

Fig. 3. Raman spectrum of pyrrole-β-cyclodextrin conjugate monomer (A), polymer spectrum type I (B) and type II (C).

the polymer (Figure 3B, C) prepared by electrochemical polymerization onto a Pt/Au-plate were compared. Because of possible inhomogeneity of the polymeric layer on the metallic substrate, simple spectral mapping (8 points) was used. The obtained spectra can be divided into two groups exhibiting distinct spectral patterns. The first group, designated as spectrum type I, (Figure 3B) shows a similar band in the range of the C–H stretching vibration to the spectrum of the monomer (Figure 3A) while the second group, designated as spectrum type II (Figure 3C), differs very significantly. Interpretation of the bands in all collected Raman spectra was performed empirically based on their assignment to the characteristic bands of functional groups/skeletons using literature data [23–24]. We should note that the spectra of both groups informed us about the very distinct arrangement of the polymeric layer derived from PPy-β-CD onto the metallic substrate. The polymer spectrum type I exhibited a relatively narrow band characteristic of β-CD at 2901 cm^{-1} assigned to the CH groups of β-CD (Figure 3B). The clearly distinguishable bands at 1124, 1094, 1475, 1432 and 1385 cm^{-1} were assigned to the several ν(C–O) and δ(CH_2) modes, respectively. Hence, the spectra confirmed the presence of β-CD. On the other hand, the band appearing at ca. 1608 cm^{-1} was assigned to the plane vibrations of the pyrrole rings. The out-of-plane modes of the pyrrole ring were observed as weak bands at ca. 958 cm^{-1} and 949 cm^{-1}, which can be attributed to almost parallel orientation of pyrrole ring with the metallic surface [25–26].

The polymer spectrum type II differed substantially from both the spectrum of the monomer and the polymer spectrum type I. In the spectrum type II (Figure 3C), the broad bands characteristic of in-plane vibrations of the pyrrole ring, namely, 1597 cm^{-1} and 1620 cm^{-1}, were slightly shifted and relatively intensified compared to the monomer (Figure 3A). Further pyrrole ring bands (e.g. at 1380 cm^{-1} of pyrrole C–N group and at 969 cm^{-1} attributed to out-of-plane vibration) were more intense than the bands characteristic of β-CDs indicating the close vicinity of pyrrole rings to the metal surface. The evident band shifts and changes of band shapes for pyrrole vibrational modes compared both to monomer and polymer type I are explained by an interaction of adsorbed pyrrole units with Au surface in the case of polymer type II.

Simultaneously, these spectral features indicate some disordering of the polymer chain system deposited on the Pt/Au metallic substrate.

We can summarize that the layer is composed of two different forms, the polymer arrangement of type I exhibits i) a higher degree of ordering and interaction of β-CD units with Pt/Au in the deposited polymeric film and ii) relatively less significant contribution of pyrrole units compared to the arrangement of type II, which exhibit i) a low degree of order of polymer chains and ii) a significant interaction of pyrrole rings with the Pt/Au metallic substrate (see above).

The morphology of the Au surface before (Figure 4A) and after the deposition of PPy-β-CD (Figure 4B) was characterized by SEM. Due to the very low roughness of the Au surface and the proper grounding, it was possible to suppress charging effects and take micrographs of the bare and PPy-β-CD-modified Cr/Au surface without any additional deposition of the conducting film. As shown in Figure 4A, the Cr/Au surface is a very dense flat structure with visible surface texture with dimensions of ~30 nm. After the deposition of PPy-β-CD (Figure 4B), cone/ball-shaped structures with diameters from 50 to 200 nm were observed on the surface. These structures are homogeneously distributed across the whole surface and are distant from each other ~400 nm (Figure 4C). The AFM imaging results showed the same morphology as SEM. The structures of PPy-β-CD on the gold surface differ in adhesion, conductivity, and surface potential (see Supporting Information, Figures 1s, 2s, 3s).

In summary, the spectroscopic results independently confirm that the PPy-β-CD polymeric layer was present as the cone/ball-shaped structures uniformly arranged over the entire surface.

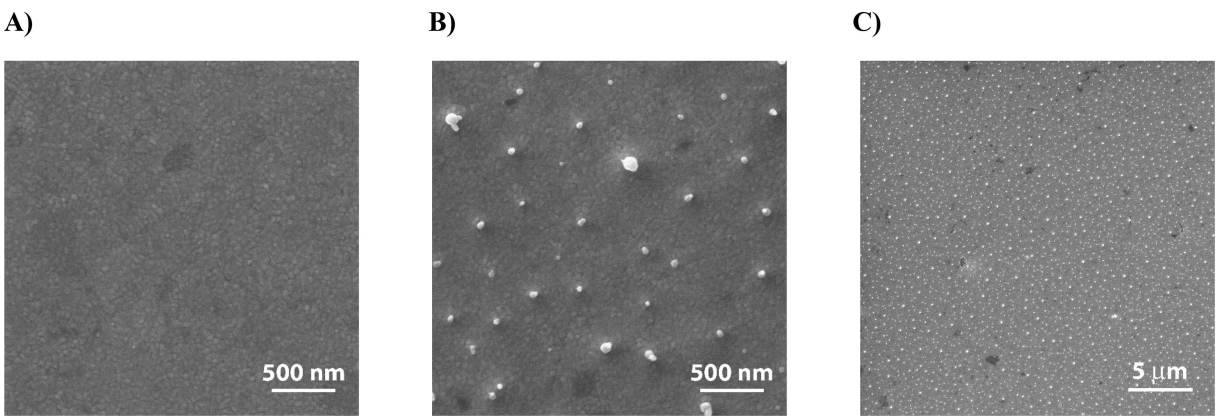

Fig. 4. SEM micrographs of gold surface before (A; magnification 100 k×) and after electrochemical deposition of pyrrole-β-cyclodextrin conjugate (B and C with 100 k× and 10 k× magnification, respectively).

3.3 Molecular Recognition

In order to assess the recognizing properties of PPy-β-CD deposited onto a solid surface towards enantiomers of Phe, LSV and QCM experiments were additionally carried out. According to the obtained spectroscopic results, the recognizing process could be affected by both the β-CD units arranged on the solid electrode surface and the areas uncoated by the polymeric layer. From our perspective, combining LSV and QCM techniques should provide insight into the possible mechanism of binding.

Figure 5 depicts the LSV responses towards L-Phe (left column) and D-Phe (right column) of a bare GCE before and after the electrodeposition of native (PPy) and substituted (PPy-β-CD) pyrrole. Here it is important to note that voltammetric discrimination can be based both on the change in peak current and the difference between peak potentials observed in the solutions of enantiomers [27–29].

For the bare GCE, the peak current intensity and the difference between the peak potentials of the redox marker were insignificant (Figure 5A–B). For the PPy-modified GCE, it was difficult to compare the intensity of the broad and not easily distinguishable peak, whose intensity visibly lost height with every addition of L- and D-Phe (Figure 5C–D). For the PPy-β-CD-modified GCE (Figure 5E–F), we observed both improvements in the peak form and concentration dependences towards Phe enantiomers compared to the PPy-modified GCE. The PPy-β-CD-modified GCE fulfilled our expectations in terms of the changes in current signal and shift in peak potentials for the redox marker.

As shown in Table 1, the PPy and PPy-β-CD-modified GCE responded in different ways to the changes in concentration of the added amino acid methyl ester. Differences were first of all observed between the signs and values of sensitivity towards Phe enantiomers for the tested GCEs. Firstly, the sensitivity for PPy-β-CD-modified GCE was positive, while the sensitivity for the PPy-modified GCE was negative. Secondly, while the sensitivity for L- and D-Phe was the same for the PPy-modified GCE, a higher sensitivity toward D-Phe than for L-Phe was obtained with the PPy-β-CD-modified GCE. With the PPy-modified GCE, the observed signal results from unspecific sorption that can not guarantee the discrimination of the amino acid methyl esters in question.

The effects observed on a PPy-β-CD-modified GCE can be considered to be confirmation of the presence and functionality of selective β-CD units attached by electrochemical oxidation of pyrrole onto the electrode surface. Moreover, our statement can be supported by the results of Gao et al. who investigated L- and D-Phe recognition using β-CD deposited onto a sp^3-to-sp^2 converted regenerative graphene/diamond (G/D) electrode [30]. However, it is difficult to agree with the statements in [30], that the electrochemical signal is the result of the oxidation of Phe enantiomers (E_{ox}(L-Phe) = 576 mV, E_{ox}(D-Phe) = 550 mV). Unfortunately, the authors did not discuss the mechanism of binding of the Phe enantiomers by β-CD onto the G/D surface and the group responsible for the observable electrochemical signal. Our attempts to obtain an electrochemical signal without a redox marker were unsuccessful. Therefore, we proposed that the redox marker is playing an important role in the formation of the signal as a result of the recognition process that occurred at the PPy-β-CD-modified GCE.

Further, this was followed by a series of QCM experiments to provide quantitative information on the amount of adsorbed enantiomers of phenylalanine methyl ester hydrochlorides on the bare and PPy-β-CD-modified surface. When comparing the adsorbed mass (Table 2), L-Phe has a higher affinity towards the electrode area, where it is able to combine both nonspecific (present at the uncoated area) and specific interactions (present at PPy-β-CD-modified area). Otherwise, L-Phe acts as a surface insulator and electron transfer inhibitor.

3.4 Mechanism of Recognition

Spectroscopic and electrochemical studies showed that a surface modified with PPy-β-CD has both uncoated and coated areas. We propose that highly ordered β-CD units distributed near the surface form inclusion complexes with enantiomers, while uncoated areas of the surface support electron exchange of the redox marker (Scheme 1). Recently, special attention was paid to the $[Fe(CN)_6]^{4-}/[Fe(CN)_6]^{3-}$ non-ideal heterogeneous charge transfer mechanism [31–32]. This has led to the proposal of the existence of an activated complex formed between the cation and the complex anion which is already paired to at least one other cation. As can be observed, the increasing concentration of D-Phe led to an increase in the electrochemical signal. This phenomenon should occur if a negatively charged redox marker compensates the

Table 1. Comparison of sensitivity obtained with bare and modified glassy carbon electrodes in supporting electrolyte (5.0 mM $K_3[Fe(CN)_6]/K_4[Fe(CN)_6]$ (1 : 1) + 0.1 M $LiClO_4$) plus the different concentrations of the amino acid methyl ester hydrochloride in question.

Analyte	GCE electrode sensitivity ($\times 10^3$) (n = 3)		
	Bare	PPy-modified	PPy-β-CD-modified
L-Phe	11	−22	6 ± 1
D-Phe	18	−28	138 ± 15

Table 2. Sorption of enantiomers of phenylalanine methyl ester hydrochlorides onto bare and PPy-β-CD-modified surface studied using quartz crystal microbalance.

Analyte	Bare Mass (ng/cm^2)	PPy-β-CD-modified Mass (ng/cm^2)
L-Phe	350	6406
D-Phe	17	2016

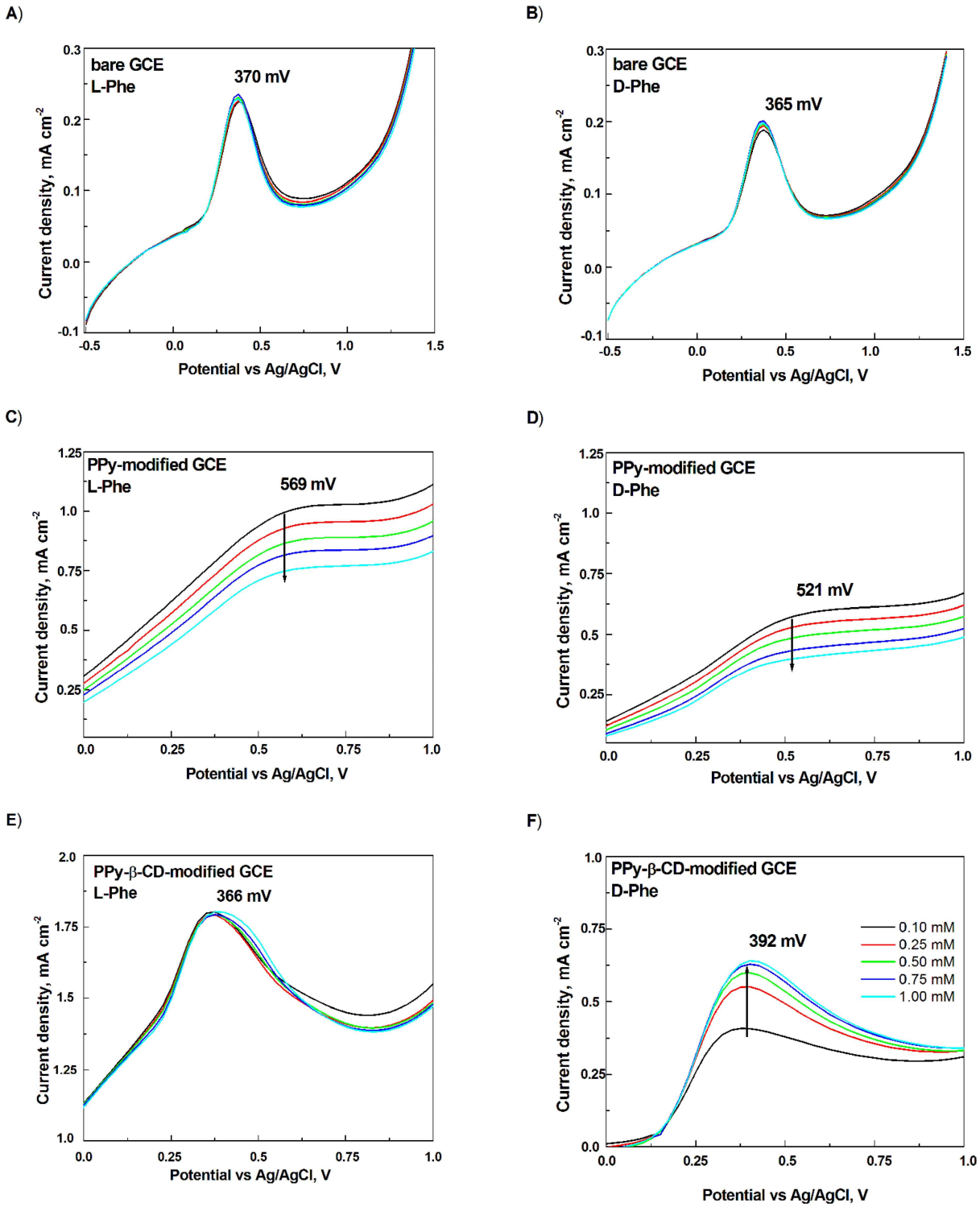

Fig. 5. Linear sweep voltammetry measurement obtained with glassy carbon electrode before modification (A, B) and after modification with unsubstituted pyrrole (PPy; C–D), a poly(pyrrole-β-cyclodextrin conjugate) (PPy-β-CD; E–F) in the supporting electrolyte containing 5.0 mM $K_3[Fe(CN)_6]/K_4[Fe(CN)_6]$ (1:1) changes the concentration of phenylalanine methyl ester enantiomers (L-Phe left side; D-Phe right side).

positive charge located on the amino group of the bound D-Phe methyl ester hydrochloride. The situation in which the electrochemical signal does not change with the increasing concentration of L-Phe is likely if the positively charged $-NH_3^+$ of L-Phe methyl ester hydrochloride is hidden in the inner β-CD cavity [29] and is, therefore,

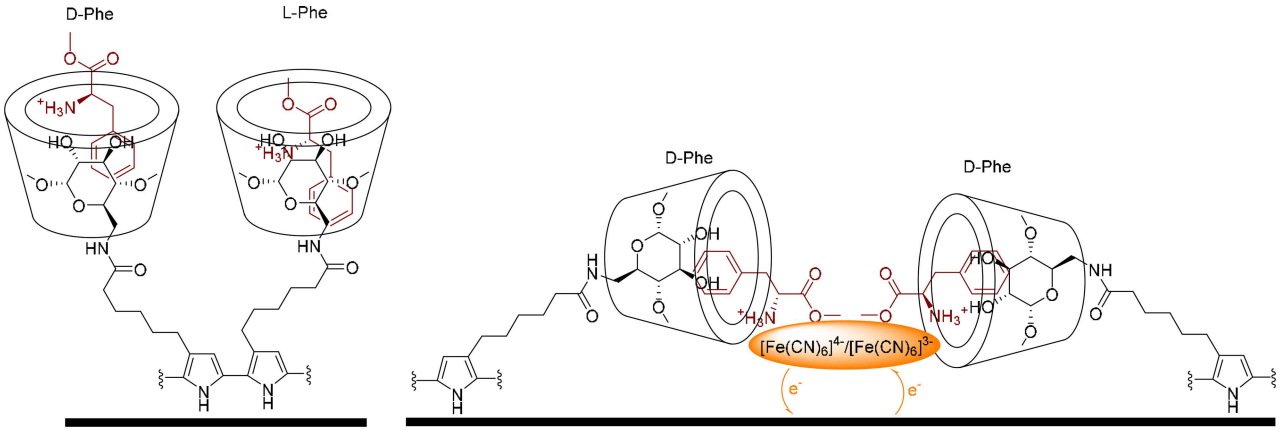

Scheme 1. Possible mechanism of molecular recognition of methyl ester hydrochloride of phenylalanine onto surface modified with pyrrole-β-cyclodextrin conjugate.

unavailable for the redox marker (Scheme 1). This observation is in agreement with previously published results [33–35].

4 Conclusion

In this work, a polymer layer based on PPy-β-CD was deposited onto solid surfaces using cyclic voltammetry. The results from both the SERS and SEM measurements confirm that the PPy-β-CD polymeric layer is comprised of cone/ball-shaped structures uniformly arranged over the entire surface. Moreover, the PPy-β-CD polymeric layer consists of differently ordered β-CD units and pyrrole rings near the solid surface that are responsible for its ability to react by various means towards enantiomers of phenylalanine methyl ester hydrochlorides. The combination of LSV and QCM measurements provided insight into the mechanism binding enantiomers onto the PPy-β-CD modified solid surface. While L-Phe acts as a surface insulator and electron transfer inhibitor, D-Phe creates a complex with $[Fe(CN)_6]^{4-}/[Fe(CN)_6]^{3-}$ and facilitates electron transfer. We are currently working on improving the electroanalysis by taking advantage of the possibilities of chemometrics.

Acknowledgements

This research was supported by a specific university research grant (Ministry of Education, Youth and Sports of the Czech Republic UCT Prague, CZ, 402850055) and within the framework of National Sustainability Program II (Ministry of Education, Youth and Sports of the Czech Republic, Project BIOCEV-FAR, reg. no. LQ1604). Přemysl Fitl and Martin Vrňata acknowledge the Grant Agency of the Czech Republic (Project No. 18-09347S), Ministry of Education, Youth and Sports within the project LTC17058 and COST Action CA15107 Multi-Comp.

References

[1] L. Liu, Q.-X. Guo, *J. Inclusion Phenom. Macrocyclic Chem.* **2002**, *42*, 1–14.
[2] L. Szente, E. Fenyvesi, *Mater. Struct. Chem.* **2017**, *28*, 479–492.
[3] A. Abbaspour, A. Noori, *Biosens. Bioelectron.* **2011**, *26*, 4674–4680.
[4] G. Zhu, Y. Yi, J. Chen, *Trend Anal. Chem.* **2016**, *80*, 232–241.
[5] W. Kutner, W. Storck, K. Doblhofer, *J. Inclusion Phenom.* **1992**, *13*, 257–265.
[6] W. Kutner, K. Doblhofer, *J. Electroanal. Chem.* **1992**, *326*, 139–160.
[7] W. Kutner, *Electrochim. Acta* **1992**, *37*, 1109–1117.
[8] D. L. Dermody, R. F. Peez, D. E. Bergbreiter, R. M. Crooks, *Langmuir* **1999**, *15*, 885–890.
[9] L. Zheng, S. Wu, X. Lin, L. Nie, L. Rui, X. Yang, *Macromolecules* **2002**, *35*, 6174–6177.
[10] F. Zhang, S. Gu, Y. Ding, Z. Zhang, L. Li, *Anal. Chim. Acta* **2013**, *770,* 53–61.
[11] F. Shang, L. Zhou, K. A. Mahmoud, S. Hrapovic, Y. Liu, H. A. Moynihan, J. D. Glennon, J. H. T. Luong, *Anal. Chem.* **2009**, *81*, 4089–4098.
[12] W. Chen, X. Wan, N. Xu, G. Xue, *Macromolecules* **2003**, *36*, 276–278.
[13] T. Sen, S. Mishra, N. G. Shimpi, *Mater. Sci. Eng. B* **2017**, *220*, 3–21.
[14] N. Izaoumen, D. Bouchta, H. Zejli, M. E. Kaoutit, A. M. Stalcup, K. R. Temsamani, *Talanta* **2005**, *66*, 111–117.
[15] G. P. Evans, *Advances in Electrochemical Science and Engineering, vol. 1, Verlag Chemie, Weinheim* **1990**.
[16] J. Lukášek, M. Řezanková, I. Stibor, M. Řezanka, *J. Inclusion Phenom. Macrocyclic Chem.* **2018**, *92*, 339–346.
[17] O. Volochanskyi, M. Švecová, V. Prokopec, *Spectrochim. Acta Part A* **2019**, *207*, 143–149.
[18] M. Lemaire, R. Garreau, J. Roncali, D. Delabouglise, H. K. Youssoufi, F. Gamier, *New J. Chem.* **1989**, *13*, 863–871.
[19] R. J. Waltman, J. Bargon, *Can. J. Chem.* **1986**, *64*, 76–95.
[20] Y. Wei, G. W. Jang, C. C. Chan, K. F. Hsueh, R. Hariharan, S. A. Patel, C. K. Whitecar, *J. Phys. Chem.* **1990**, *94*, 7716–7721.
[21] M. Saraji, A. Bagheri *Synth. Met.* **1998**, *98*, 57–63.
[22] J. Arjomandi, R. Holze, *J. Solid State Electrochem.* **2007**, *11*, 1093–1100.
[23] O. Egyed, *Vib. Spectrosc.* **1990**, *1*, 225–227.

[24] J. Arjomandi, A.-u.-H. A. Shah, S. Bilal, H. V. Hoang, R. Holze, *Spectrochim. Acta Part A* **2011**, *78*, 1–6.
[25] M. Moskovits, *J. Chem. Phys.* **1982**, *77*, 4408.
[26] E. L. Ru, P. Etchegoin, *Principles of Surface-Enhanced Raman Spectroscopy, Elsevier Science* **2008**.
[27] M. Trojanowicz, *Electrochem. Commun.* **2014**, *38*, 47–52.
[28] S. Ates, E. Zor, I. Akin, H. Bingol, S. Alpaydin, E. G. Akgemci, *Anal. Chim. Acta* **2017**, *970*, 30–37.
[29] S. A. Zaidi, *Biosens. Bioelectron.* **2017**, *94*, 714–718.
[30] J. Gao, H. Zhang, C. Ye, Q. Yuan, W. K. Chee, W. Su, A. Yu, J. Yu, C.-T. Lin, D. Dai, L. Fu, *Nanomaterials* **2018**, *8*, 1050.
[31] D. J. Blackwood, S. Pons, *J. Electroanal. Chem.* **1988**, *244*, 301–305.
[32] L. M. Peter, W. Durr, P. Bindra, H. Gerischer, *J. Electroanal. Chem.* **1976**, *71*, 31–50.
[33] X. Niu, Z. Mo, X. Yang, C. Shuai, N. Liu, R. Guo, *Bioelectrochemistry* **2019**, *128*, 74–82.
[34] J. M. Alexander, J. L. Clark, T. J. Brett, J. J. Stezowski, *PNAS* **2002**, *99*, 5115–5120.
[35] R. Freeman, T. Finder, L. Bahshi, I. Willner, *Nano Lett.* **2009**, *9*, 2073–2076.

Received: October 11, 2019
Accepted: November 19, 2019
Published online on ■■, ■■

FULL PAPER

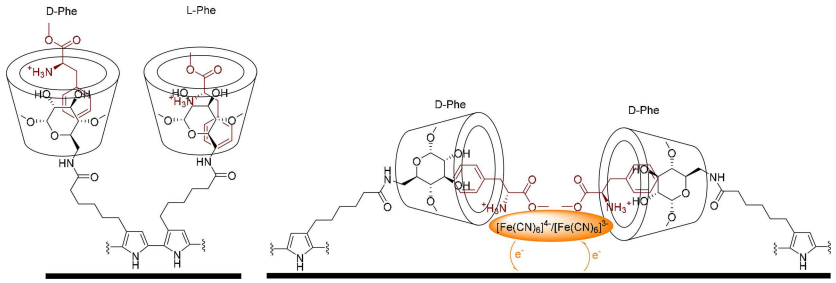

T. V. Shishkanova, N. Habanová, M. Řezanka, G. Broncová, P. Fitl, M. Vrňata, P. Matějka*